Green Chemistry

ROYAL SOCIETY OF CHEMISTRY

PAPER

View Article Online
View Journal | View Issue

Check for updates

Cite this: *Green Chem.*, 2023, **25**, 8791

Open Access Article. Published on 29 September 2023. Downloaded on 7/19/2025 6:26:52 PM. This article is licensed under a Creative Commons Attribution 3.0 Unported Licence.

Cation–anion confined hydrogen-bonding catalysis strategy for ring-closing C–O/O–H metathesis of alkoxy alcohols under metal-free conditions†

Huan Wang,‡[a,b] Zhi-Hao Zhao,‡[a,d] Yanfei Zhao,[a,c] Fengtao Zhang,[a,c] Junfeng Xiang,[a] Buxing Han [a,c] and Zhimin Liu *[a,c]

Received 14th August 2023,
Accepted 25th September 2023

DOI: 10.1039/d3gc03041e

rsc.li/greenchem

Ring-closing metathesis (RCM) reactions of multiple bonds have seen considerable progress; however, RCM reactions involving single bonds, especially two different single bonds are scarce and extremely challenging. Herein, we present a cation–anion confined hydrogen bonding catalysis strategy for catalyzing the ring-closing C–O/O–H metathesis of alkoxy alcohols to O-heterocycles under metal-free conditions. Assisted with theoretical computation, the effective ionic liquid catalysts were first predicted. [HO-EtMIm][OTf] was found to display the highest activity, consistent with the predicted results. This catalyst could afford a series of O-heterocycles, including tetrahydrofurans, tetrahydropyrans, dioxanes, and some complex ethers that are difficult to access *via* conventional routes. Moreover, it was recyclable and reusable without activity loss after 5 recycles. Comprehensive investigations endorse that $[HO\text{-}EtMIm]^+$ cation and $[OTf]^-$ anion selectively form hydrogen bonds with the ether O atom and hydroxyl H atom of alkoxy alcohol in opposite directions, respectively, which cooperatively catalyze the reaction in the cation–anion confined ionic microenvironment. The strategy presented here provides a novel and green route to access cyclic ethers.

Introduction

Metathesis reactions are widely applied to synthesize complex molecules, pharmaceuticals, and natural products.[1–7] Particularly, ring-closing metathesis (RCM) reactions of multiple bonds, such as olefin-olefin metathesis[2,8–11] and carbonyl-olefin metathesis[5,12–16] have become powerful techniques for the preparation of various unsaturated rings in organic synthesis (Scheme 1a and b). In contrast, the RCM reactions of the C–X bond especially involving the C–O bond are rarely reported and still challenging owing to the low reactivity of single bonds.[17–22] Recently, it has been reported that Lewis acid (*e.g.*, $Fe(OTf)_3$) and SO_3H-functionalized ILs are capable of catalyzing ring-closing C–O/C–O bond metathesis reactions of aliphatic ethers to bis- and tris-ethers,[13,23] and silicon could catalyze C–O bond RCM of polyethers.[19] Notably, these RCM systems only involve the transformation of the substrates with two same single bonds (*e.g.*, C–O bond). Compared to sym-

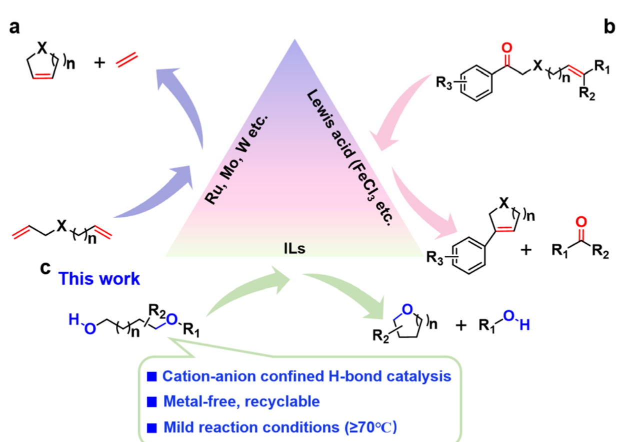

Scheme 1 Ring-closing metathesis reactions.

[a]Beijing National Laboratory for Molecular Sciences, Key Laboratory of Colloid and Interface and Thermodynamics, Institute of Chemistry, Chinese Academy of Sciences, Beijing 100190, China. E-mail: liuzm@iccas.ac.cn
[b]College of Chemistry & Chemical Engineering, Shaanxi Key Laboratory of Chemical Additives for Industry, Shaanxi University of Science & Technology, Xi'an, Shaanxi, 710021, China
[c]University of Chinese Academy of Sciences, Beijing 100049, China
[d]State Key Laboratory of Solidification Processing and School of Materials Science and Engineering, Northwestern Polytechnical University, Xi'an, Shaanxi, 710072, P. R. China

† Electronic supplementary information (ESI) available. See DOI: https://doi.org/10.1039/d3gc03041e

‡ These authors contributed equally.

Open Access Article. Published on 29 September 2023. Downloaded on 7/19/2025 6:26:52 PM. This article is licensed under a Creative Commons Attribution 3.0 Unported Licence.

metrical compounds, asymmetric compounds are more difficult to be activated and transformed, and the catalytic system with two different active sites is usually required. The ring-closing C–O/O–H metathesis of alkoxy alcohols remains challenging and has not been reported so far, and therefore an efficient and green strategy for this reaction is highly desirable (Scheme 1c).

Since the past decades, ionic liquids (ILs) composed of organic cations and organic/inorganic anions have been emerging as promising alternatives to metal catalysts due to their unique properties such as structural designability, negligible volatility, strong H-bonding interactions, and easy recycling.[24–29] Particularly, the strong hydrogen bonding interactions in IL systems make them show promising applications in catalyzing reactions under metal-free and mild conditions.[30–35] For example, acetate-[36] or trifluoroethanol-[37] based ILs could activate 2-aminobenzonitriles *via* hydrogen bonding, thus catalyzing the reaction of CO_2 with 2-aminobenzonitriles to quinazoline-2,4(1*H*,3*H*)-diones. Basic IL 1-ethyl-3-methylimidazolium acetate could catalyze the one-pot oxidative esterification of alcohols using O_2 as an oxidant under catalysis of hydrogen bonding interaction.[38] The cooperation of the IL cation as hydrogen bond (HB) donor and anion as acceptor could efficiently achieve dehydrative cyclization of diols to O-heterocycles.[39]

In this work, we for the first time report the ring-closing C–O/O–H bonds metathesis of alkoxy alcohols to O-heterocycles achieved over OH-functionalized ILs (Scheme 1 and Fig. S1†). Assisted with theoretical computations, the proper range of IL hydrogen bonding catalysts was first predicted. [HO-EtMIm][OTf] (1-hydroxyethyl-3-methyl imidazolium trifluorom-ethanesulfonate) was found to be very effective for the reaction, agreeing well with the prediction. A series of O-heterocycles including tetrahydrofurans, tetrahydropyrans, dioxanes, and some other complex ethers can be produced in high yields using this strategy. Comprehensive investigations indicate that a pair of cation and anion of [HO-EtMIm][OTf] serve as HB donor and acceptor (D–A), respectively, to form strong HBs with a molecule of 1,4-butanediol monomethyl ether (**1a**), which selectively activate the C–O and O–H bonds, thus synergistically catalyzing the transformation of alkoxy alcohol to cyclic ethers in the cation–anion confined electroneutral microenvironment.

Results and discussion

Taking **1a** as a model of alkoxy alcohols, we set out to select the ILs with cation and anion as HB donor and acceptor, respectively, through density functional theory (DFT) calculations. Considering that the strengths of HBs between the cations or anions of ILs and the reactant reflect the activity of the IL catalyst in our previous work,[23,39] we performed DFT calculations to estimate the lengths of HBs between **1a** and various cations or anions, respectively. As shown in Fig. 1a and S2,† the cations $[HO\text{-}EtN_{111}]^+$, $[HO\text{-}EtMIm]^+$, and $[EMIm]^+$ serve as HB donors to form HBs with the ether O atom of **1a** with the HB lengths following the order: $[HO\text{-}EtN_{111}]^+ < [HO\text{-}EtMIm]^+ < [EMIm]^+$; especially, the HB lengths of **1a** with $[HO\text{-}EtN_{111}]^+$ and with $[HO\text{-}EtMIm]^+$ are less than 2.0 Å, suggesting very strong hydrogen bonding interaction.[40,41] The anions $[OTf]^-$, $[PF_6]^-$, Cl^- serve as HB acceptors to form HBs with the hydroxyl H of **1a**, and the HB lengths are as follows: $[OTf]^- < [PF_6]^- < Cl^-$, indicating the strongest ability of $[OTf]^-$

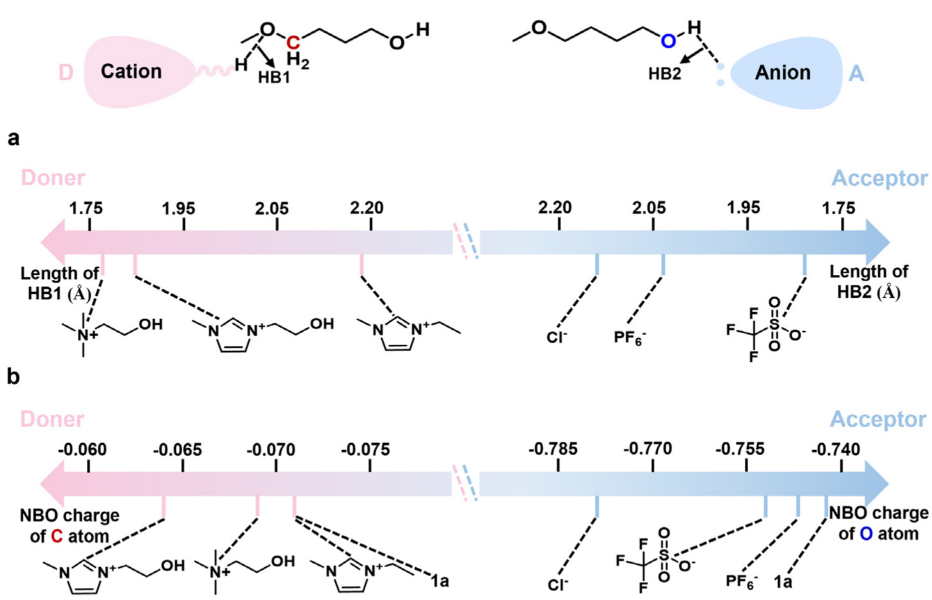

Fig. 1 Hydrogen bonding interaction of **1a** with various cations or anions. (a) The lengths of HBs between **1a** and various cations or anions, respectively; (b) the natural bond orbital (NBO) charges of methylene C atom of $-CH_2OCH_3$ and hydroxyl O atom in **1a** when **1a** interacts with and without various cations or anions, respectively.

 This journal is © The Royal Society of Chemistry 2023

Open Access Article. Published on 29 September 2023. Downloaded on 7/19/2025 6:26:52 PM. This article is licensed under a Creative Commons Attribution 3.0 Unported Licence.

to form HB with **1a**. Additionally, the NBO charges of the methylene C atom in –CH_2OCH_3 and the hydroxyl O atom in **1a** were calculated to get information on electron transfer caused by hydrogen bonding (Fig. 1b and S2†). Compared to those of **1a**, both NBO charges of methylene C atom in –CH_2OCH_3 and hydroxyl O atom in **1a** change remarkably as **1a** interacts with these cations or anions, following the order: $[EMIm]^+ < [HO\text{-}EtN_{111}]^+ < [HO\text{-}EtMIm]^+$ and $[PF_6]^- < [OTf]^- < Cl^-$, respectively. From the above results, it is obvious that all the selected cations and anions can interact with **1a** *via* hydrogen bonding interaction, which results in changes in the NBO charges of methylene C atom in –CH_2OCH_3 and hydroxyl O atom in **1a** accordingly. Therefore, it may be deduced that a pair of cation and anion could jointly interact with **1a** *via* hydrogen bonding due to the presence of electrostatic force. It is generally accepted that the shorter the HB length, the stronger the hydrogen bonding interaction, and that the larger change in the NBO charge suggests more electron transfer. Hence, the ILs composed of OH-functionalized cation and anion containing halogen/O atoms may be capable of catalyzing the RCM of **1a**.

Based on the calculated results, we selected the ILs composed of the above cations and anions to examine their catalytic activities for **1a** RCM (Fig. 2a). To our delight, the ILs with $[OTf]^-$ anion and –OH functionalized cations, *e.g.*, [HO-EtMIm][OTf], [HO-EtMMIm][OTf] and [HO-EtN_{111}][OTf], were very effective for the reaction, even better than the commonly applied H_2SO_4 (22 wt%) catalyst. Especially, [HO-EtMIm][OTf] showed the best performance, generating tetrahydrofuran (**1b**) as the sole product with an excellent yield of 91% and an *E* factor of 0.44[42] (Fig. 2a and S3†). To explore the stability of **1a** under the experimental conditions, the reaction of **1b** with MeOH was tried, and no **1a** was detected, suggesting that the formation of **1b** was irreversible (Fig. S4†).

However, the OH-functional ILs with other anions, including [HO-EtMIm][NTf_2], [HO-EtMIm][BF_4], [HO-EtMIm][PF_6], [HO-EtMIm][Cl], [HO-EtMIm][NO_3], [HO-EtMIm][OTs], [HO-EtMIm][$N(CN)_2$] and [HOEtMIm][ClO_4] were ineffective (Fig. 2a), suggesting that the $[OTf]^-$ anion of the effective ILs played an important role in this reaction. On the other hand, the presence of –OH in the cation was also crucial deduced from the fact that the reaction did not occur using [EtMIm][OTf] as the catalyst (Fig. 2a). In comparison, the experimental results worked out to be consistent with the calculated prediction. The cooperation of the cation and anion of the IL is responsible for the catalytic performance. Additionally, Brønsted acid IL [HO-EtMIm][HSO_4] was also examined for this reaction, showing much lower activity than [HO-EtMIm][OTf]. CH_3COOH that has a similar pK_a value to [HO-EtMIm][OTf][39] was found to be ineffective. These findings suggest that the RCM reaction of **1a** may not follow an acid-catalysis mechanism. Notably, no 1-methoxy-4-(4-methoxybutoxy)butane was detected in the reaction solution, indicating that no intermolecular dehydration reaction of **1a** occurred, which may be attributed to the cation–anion confinement effect. In addition, NaOTf was examined as a catalyst, and no **1b** was obtained, implying that the effect of the residual metal (Na^+, 0.012 wt%) in the ILs on this reaction could be negligible (Fig. 2a).

Subsequently, the effects of temperature, the amount of IL, reaction time on the RCM of **1a** over [HO-EtMIm][OTf], and recycling test were investigated (Table S1† and Fig. 2, 3). As

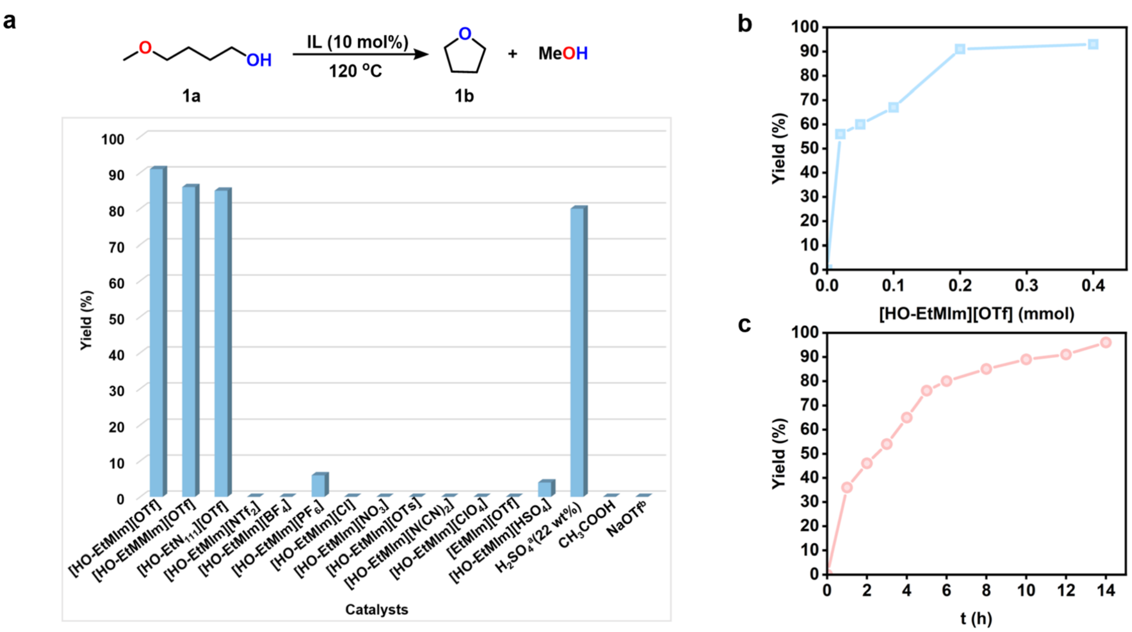

Fig. 2 Screening conditions for ring-closing metathesis of **1a**. (a) Screening for ILs; effect of (b) the catalyst loadings and (c) reaction time on the ring-closing metathesis of **1a**. Reaction conditions: **1a** (2 mmol), 120 °C of (a) 10 mol% of IL, 12 h; (b) 12 h; (c) 10 mol% of [HO-EtMIm][OTf]. [a] The amount of catalyst was based on H_2SO_4. [b] 10 mol% of NaOTf, *n*-hexane (0.45 M). Yields were determined by ^{1}H NMR, and the data were the average of three replicates with reproducibility of ±3%.

Open Access Article. Published on 29 September 2023. Downloaded on 7/19/2025 6:26:52 PM.
This article is licensed under a Creative Commons Attribution 3.0 Unported Licence.

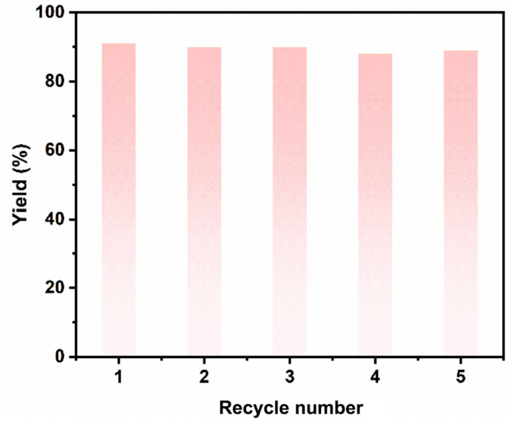

Fig. 3 The IL recycling tests for ring-closing metathesis of **1a**. Reaction conditions: **1a** (2 mmol), [HO-EtMIm][OTf] (10 mol%), 120 °C, 12 h.

shown in Table S1,† the reaction could take place even at 70 °C, and the yield of **1b** increased with temperature, achieving 94% at 140 °C within 12 h. As indicated, even with the amount of IL at 1 mol%, a high **1b** yield of 56% was still reached with a turnover frequency (TOF) of 112 h^{-1} (Fig. 2b); a **1b** yield of 36% was obtained within 1 h at 120 °C, and it reached up to 96% for 14 h (Fig. 2c). All these findings indicate that this catalyst was very efficient for **1a** RCM. Moreover, since [HO-EtMIm][OTf] is immiscible with product **1b**, it could be easily restored through phase separation and vacuum drying to remove the generated MeOH and unreacted **1a**. The recycling tests indicate that the product yield did not decrease obviously after the IL was reused for five runs (Fig. 3). The ^{1}H and ^{19}F NMR spectra of IL before and after the reaction remained unchanged (Fig. S5 and S6†). These results indicate that this IL has good stability and reusability under experimental conditions. Notably, a small amount of dimethyl ether was obtained, which was originated from the dehydrative etherification of the generated MeOH during the reaction process (Fig. S3†).[39]

Under the optimized experimental conditions, the RCM reactions of a series of alkoxy alcohols over [HO-EtMIm][OTf] were conducted. As illustrated in Table 1 and Fig. S7–10,† five- and six-membered aliphatic and aromatic O-heterocycles were produced in high yields from 81% to ~99% in most cases under similar experimental conditions (**1b–4b**). However, only a 50% yield of **5b** was obtained, probably due to the steric hindrance effect of **5a**. 1,4-Dioxane (**6b**), dimethyl-substituted 1,4-dioxane (**7b**) as well as 3-hydroxytetrahydrofuran (**8b**) that are usually applied in drug design were also obtained in good yields. It should be pointed out that no byproducts from intermolecular dehydration of alkoxyl alcohols were detectable during the above reactions, although [HO-EtMIm][OTf] performed well in catalyzing the intermolecular dehydration of alcohols in our previous study.[39] This supports the cation–anion confinement effect on the RCM reactions of alkoxyl alcohols.

Clearly, OH-functional ILs with $[OTf]^-$ anion are suitable catalysts for the RCM reactions of alkoxyl alcohols according

Table 1 Substrate scope

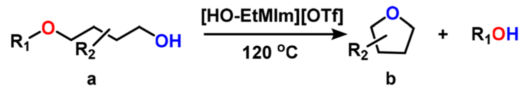

Substrate		Product	
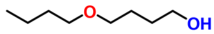	1a'	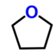	1b, >99%[a]
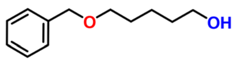	2a	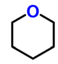	2b, 81%[b]
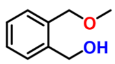	3a	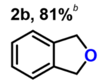	3b, >99%[c]
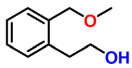	4a	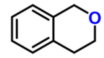	4b, >99%[c]
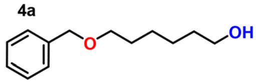	5a	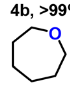	5b, 50%[b]
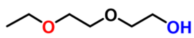	6a	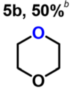	6b, >99%[b]
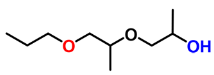	7a	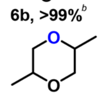	7b, 82%[c]
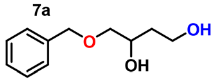	8a	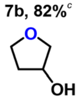	8b, 80%[c]

Reaction conditions: alkoxy alcohol 1 mmol, 10 mol% of [HO-EtMIm][OTf]. [a] 36 h. [b] 48 h. [c] 50 mol% of [HO-EtMIm][OTf], 48 h. Yields were determined by ^{1}H NMR.

to either the DFT prediction or the experimental results. However, why do both anion and cation of the IL have such an important effect on this reaction, and how do the anion and cation of the IL synergistically catalyze reactions?

To answer these questions, the hydrogen bonding interaction between these ILs and **1a** was investigated by DFT calculations and NMR analysis. For comparison, five ILs including [HO-EtMIm][OTf], [HO-EtMMIm][OTf], [$HOEtN_{111}$][OTf], [HO-EtMIm][Cl] and [EMIm][OTf] were selected to perform the DFT calculations. From the optimized figurations of these ILs interacting with **1a** (Fig. 4 and S11†), it is obvious that **1a** could form dual HBs with both the cation and anion of the ILs. The estimated lengths of HBs between the ether O atom of **1a** and the hydroxyl H or C2–H in the cations are 1.77 Å for [HO-EtMIm][OTf], 1.78 Å for [$HO\text{-}EtN_{111}$][OTf], 1.80 Å for [HO-EtMMIm][OTf], 1.81 Å for [HO-EtMIm][Cl] and 2.13 Å for [EMI-m][OTf], meanwhile, those of HBs between the hydroxyl H atom of **1a** and the O atom in $[OTf]^-$ or Cl^- atom are estimated to be 1.86 Å, 1.91 Å, 1.93 Å, 1.97 Å and 2.13 Å for [$HO\text{-}EtN_{111}$][OTf], [EMIm][OTf], [HO-EtMIm][OTf], [HO-EtMMIm][OTf] and [HO-EtMIm][Cl], respectively. These results demonstrate that as the HB donor the OH-functiona-

 This journal is © The Royal Society of Chemistry 2023

Open Access Article. Published on 29 September 2023. Downloaded on 7/19/2025 6:26:52 PM.
This article is licensed under a Creative Commons Attribution 3.0 Unported Licence.

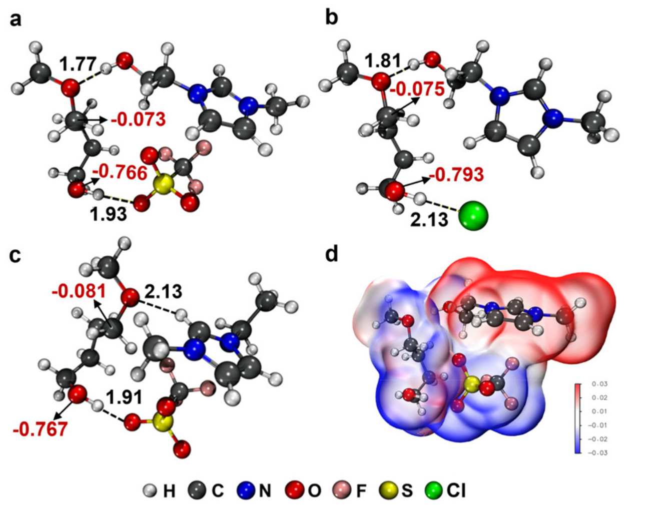

Fig. 4 DFT calculations. The interaction figurations of **1a** with ILs: (a) [HO-EtMIm][OTf], (b) [HO-EtMIm][Cl] and (c) [EMIm][OTf] optimized at M062X-D3/def2-TZVP level [black word: atom distance (Å), red word: NBO charges]; (d) ESP distribution of [HO-EtMIm][OTf] with **1a**.

lized cations including $[HO\text{-}EtMIm]^+$, $[HO\text{-}EtMMIm]^+$, and $[HO\text{-}EtN_{111}]^+$ have similar ability to form strong HBs with the ether O atom of **1a** in the presence of the $[OTf]^-$ anion, while as HB acceptor the $[OTf]^-$ anion shows a much stronger ability to form HB with hydroxyl H atom of **1a** than Cl^-. The NBO charges of the methylene C atom of $-CH_2OCH_3$ and the hydroxyl O atom in **1a** were also calculated, which changed remarkably as **1a** interacted with the ILs. The differences of NBO charges between the methylene C atom of $-CH_2OCH_3$ and the hydroxyl O atom in **1a** were estimated to be 0.718, 0.693, 0.691, 0.689 and 0.686 as **1a** interacted with [HO-EtMIm][Cl], [HO-EtMIm][OTf], $[HO\text{-}EtN_{111}][OTf]$, [HO-EtMIm] [OTf] and [EMIm][OTf], respectively (Fig. 4 and S11†). Obviously, the stronger dual hydrogen bonding interaction of the IL with **1a** and the larger difference of NBO charges may reflect the higher reactivity of **1a** under the catalysis of the IL. Therefore, it could be deduced that strong dual HBs, appropriate synergy and electrostatic confinement effect of the IL cation and anion are responsible for their catalytic activity.

Furthermore, the electrostatic potential (ESP) distribution of [HO-EtMIm][OTf] with **1a** was performed for an in-depth study on the hydrogen bonding between them (Fig. 4d). It is obvious that at the areas where the HBs are formed, the positive surface potential (red area) of –OH in $[HO\text{-}EtMIm]^+$ overlaps with the negative surface potential (blue area) of ether O atom in **1a**, meanwhile, the positive surface potential of –OH in **1a** overlaps with the negative surface potential of O atoms in $[OTf]^-$.[43–45]

Moreover, the hydrogen bonding interaction between [HO-EMIm][OTf] and **1a** was further evidenced by NMR spectroscopic experiments. As shown in Fig. 5, the chemical shift assigned to the hydroxyl H atom of $[HO\text{-}EtMIm]^+$ shifted upfield, meanwhile the signal to the ether O atom in **1a** became wider and shifted to 1.61 ppm from the initial 0.76 ppm. These results provide evidence for the formation of HB between **1a** and $[HO\text{-}EtMIm]^+$ in the form of $CH_3\text{–}(CH_2)O\cdots[HO\text{-}EtMIm]^+$, with the electron transfer from the ether O atom of **1a** to the hydroxyl H atom of $[HO\text{-}EtMIm]^+$, which may activate the ether C–O bond of $CH_3OCH_2\text{–}$ in **1a.** Meanwhile, the chemical shifts assigned to the O atoms of hydroxyl in **1a** and in the $[OTf]^-$ anion shifted from −17.26 to −18.31 ppm and from 163.31 to 163.78 ppm, respectively. The signal belonged to the hydroxyl H atom of **1a** shifted downfield, and the chemical shift of F atoms in $[OTf]^-$ shifted upfield (Fig. 5 and S12†). These results indicate that the hydroxyl H atom of **1a** may form a HB with the O atom of $[OTf]^-$ promoted by the F atoms (see ESI† for details).[46]

To get an insight into the reaction mechanism, *in situ* ^1H NMR experiments were conducted (Fig. 6 and S13†). Interestingly, two new peaks appeared at δ = 4.21 and 4.77 ppm as the reaction occurred, which are assigned to the H atom of –OMe and –OH in [HO-EtMIm]-OMe intermediate, respectively. At the beginning of the reaction, a signal appeared at 4.98 ppm, belonging to the hydroxyl H atoms in the state of **TS1**. Additionally, as the reaction proceeded, the amount of **1a** (the peaks appeared at δ = 2.00 and 3.99 ppm)

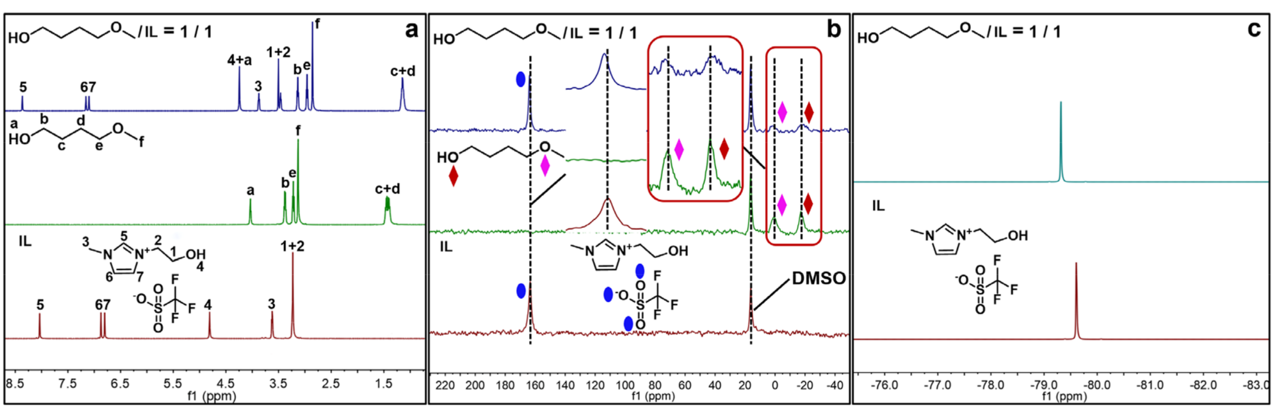

Fig. 5 NMR analysis. ^1H (a), ^{17}O (b) and ^{19}F (c) NMR spectra of [HO-EMIm][OTf], **1a** and their mixture recorded at 333.15 K.

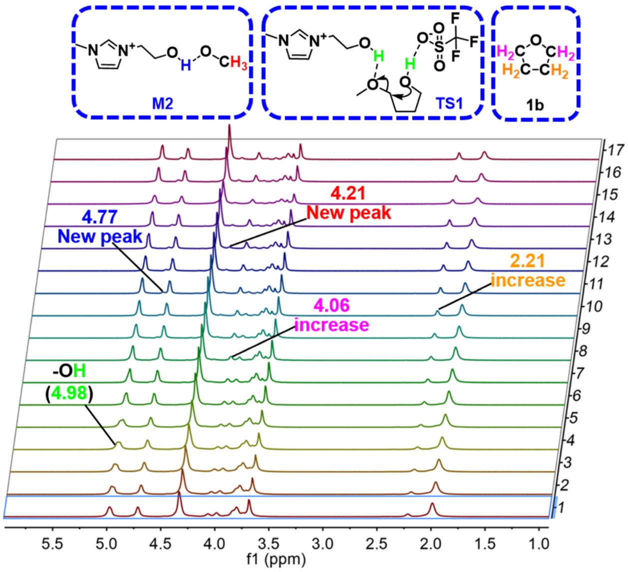

Fig. 6 The *in situ* ^{1}H NMR spectra were recorded in **1a** transformation process over [HO-EMIm][OTf] at 393.2 K.

declined with increases in the amounts of **1b** (the peaks appeared at δ = 2.21 and 4.06 ppm) and MeOH (the peak appeared at δ = 3.75 ppm) (Fig. S13†).

Based on the experimental results and previous reports,[23,39] a possible reaction pathway is proposed as illustrated in Fig. S14.† First, both C–O and O–H bonds of **1a** are simultaneously activated by a pair of IL cation and anion *via* strong H-bonding interaction. Then, the activated C atom linked to $-OCH_3$ is attacked by the activated hydroxyl O atom of **1a**, furnishing cyclic oxonium intermediate (**M1**) stabilized by the $[OTf]^-$ anion *via* the transition state of **TS1**, together with [HO-EtMIm]-OMe complex (**M2**). Finally, **2b** and MeOH are generated *via* dehydrogenation of intermediate **M1** by [HO-EtMIm]-OMe, with the regeneration of the IL.

Conclusions

In summary, assisted with DFT calculations a cation–anion confined hydrogen-bonding-catalysis strategy for ring-closing C–O/O–H bond metathesis of alkoxy alcohols to O-heterocycles is presented. [HO-EtMIm][OTf] can achieve this reaction under mild conditions, and affords various five-, six- and seven-membered aliphatic and aromatic O-heterocycles with/without alkyl, hydroxyl substituents in high yields. Mechanism studies indicate that the IL cation and anion serve as HB donor and acceptor, respectively, to form dual strong HBs with an alkoxy alcohol molecule in opposite directions, which cooperatively catalyze the reaction with high efficiency. This novel and green way to access O-heterocycles would be employed in the late-stage diversification of complex molecules and synthesis of various drugs and natural product derivatives from diverse substrates with target function groups. We believe that the cation–anion confined H-bonding catalysis strategy has promising applications in more reactions.

Author contributions

H. W. and Z. L. designed the project and prepared the manuscript for publication. H. W. and Z. Z. carried out the experiments and collected the data. Z. Z. performed the DFT calculations. All authors analyzed the data and contributed to the writing of the manuscript.

Conflicts of interest

There are no conflicts to declare.

Acknowledgements

This work was jointly supported by the Natural Science Basic Research Plan in Shaanxi Province of China (2023-JC-QN-0113), Scientific Research Plan Projects of Shaanxi Education Department (22JK0294), National Key Research and Development Program of China (2020YFA0710201), National Natural Science Foundation of China (22121002, 21890761, 22233006) and China Postdoctoral Science Foundation (2022M722597).

References

1 H. Albright, A. J. Davis, J. L. Gomez-Lopez, H. L. Vonesh, P. K. Quach, T. H. Lambert and C. S. Schindler, *Chem. Rev.*, 2021, **121**, 9359–9406.
2 X. Shen, T. T. Nguyen, M. J. Koh, D. Xu, A. W. Speed, R. R. Schrock and A. H. Hoveyda, *Nature*, 2017, **541**, 380–385.
3 A. J. Davis, R. B. Watson, D. J. Nasrallah, J. L. Gomez-Lopez and C. S. Schindler, *Nat. Catal.*, 2020, **3**, 787–796.
4 P. K. Quach, J. H. Hsu, I. Keresztes, B. P. Fors and T. H. Lambert, *Angew. Chem., Int. Ed.*, 2022, e202203344.
5 H. Albright, P. S. Riehl, C. C. McAtee, J. P. Reid, J. R. Ludwig, L. A. Karp, P. M. Zimmerman, M. S. Sigman and C. S. Schindler, *J. Am. Chem. Soc.*, 2019, **141**, 1690–1700.
6 A. Koner, B. Morgenstern and D. M. Andrada, *Angew. Chem., Int. Ed.*, 2022, **61**, e202203345.
7 M. R. Becker, R. B. Watson and C. S. Schindler, *Chem. Soc. Rev.*, 2018, **47**, 7867–7881.
8 D. L. Nascimento, A. Gawin, R. Gawin, P. A. Gunka, J. Zachara, K. Skowerski and D. E. Fogg, *J. Am. Chem. Soc.*, 2019, **141**, 10626–10631.
9 E. F. van der Eide and W. E. Piers, *Nat. Chem.*, 2010, **2**, 571–576.
10 H. F. Klare and M. Oestreich, *Angew. Chem., Int. Ed.*, 2009, **48**, 2085–2089.

Open Access Article. Published on 29 September 2023. Downloaded on 7/19/2025 6:26:52 PM.
This article is licensed under a Creative Commons Attribution 3.0 Unported Licence.

This journal is © The Royal Society of Chemistry 2023

Open Access Article. Published on 29 September 2023. Downloaded on 7/19/2025 6:26:52 PM.
This article is licensed under a Creative Commons Attribution 3.0 Unported Licence.

11 N. Lemcoff, N. B. Nechmad, O. Eivgi, E. Yehezkel, O. Shelonchik, R. S. Phatake, D. Yesodi, A. Vaisman, A. Biswas and N. G. Lemcoff, *Nat. Chem.*, 2023, **15**, 475–482.
12 C. C. McAtee, P. S. Riehl and C. S. Schindler, *J. Am. Chem. Soc.*, 2017, **139**, 2960–2963.
13 L. Ma, W. Li, H. Xi, X. Bai, E. Ma, X. Yan and Z. Li, *Angew. Chem., Int. Ed.*, 2016, **55**, 10410–10413.
14 Y. Zhang, J. Jermaks, S. N. MacMillan and T. H. Lambert, *ACS Catal.*, 2019, **9**, 9259–9264.
15 E. K. Cho, P. K. Quach, Y. Zhang, J. H. Sim and T. H. Lambert, *Chem. Sci.*, 2022, **13**, 2418–2422.
16 S. R. Todtz, C. W. Schneider, T. Malakar, C. Anderson, H. Koska, P. M. Zimmerman and J. J. Devery III, *J. Am. Chem. Soc.*, 2023, **145**, 13069–13080.
17 T. Biberger, S. Makai, Z. Lian and B. Morandi, *Angew. Chem., Int. Ed.*, 2018, **57**, 6940–6944.
18 J. Zhu, R. Zhang and G. Dong, *Nat. Chem.*, 2021, **13**, 836–842.
19 N. Ansmann, T. Thorwart and L. Greb, *Angew. Chem., Int. Ed.*, 2022, **61**, e202210132.
20 Y. Wang, J. Zhang, J. Liu, C. Zhang, Z. Zhang, J. Xu, S. Xu, F. Wang and F. Wang, *ChemSusChem*, 2015, **8**, 2066–2072.
21 Y. Ma, L. Zhang, Y. Luo, M. Nishiura and Z. Hou, *J. Am. Chem. Soc.*, 2017, **139**, 12434–12437.
22 Z. Lian, B. N. Bhawal, P. Yu and B. Morandi, *Science*, 2017, **356**, 1059–1063.
23 H. Wang, Y. Zhao, F. Zhang, Y. Wu, R. Li, J. Xiang, Z. Wang, B. Han and Z. Liu, *Angew. Chem., Int. Ed.*, 2020, **59**, 11850–11855.
24 M. Zhang, R. Ettelaie, T. Yan, S. Zhang, F. Cheng, B. P. Binks and H. Yang, *J. Am. Chem. Soc.*, 2017, **139**, 17387–17396.
25 J. Hu, J. Ma, Q. Zhu, Z. Zhang, C. Wu and B. Han, *Angew. Chem., Int. Ed.*, 2015, **54**, 5399–5403.
26 B. Wang, L. Qin, T. Mu, Z. Xue and G. Gao, *Chem. Rev.*, 2017, **117**, 7113–7131.
27 Y. Zhao, B. Han and Z. Liu, *Acc. Chem. Res.*, 2021, **54**, 3172–3190.
28 T. Yang, J. Yang, X. Deng, E. Franz, L. Fromm, N. Taccardi, Z. Liu, A. Görling, P. Wasserscheid and O. Brummel, *Angew. Chem., Int. Ed.*, 2022, **61**, e202202957.
29 S. Dongare, O. K. Coskun, E. Cagli, K. Y. Lee, G. Rao, R. D. Britt, L. A. Berben and B. Gurkan, *ACS Catal.*, 2023, **13**, 7812–7821.
30 K. Chen, G. Shi, W. Zhang, H. Li and C. Wang, *J. Am. Chem. Soc.*, 2016, **138**, 14198–14201.
31 M. Hulla, S. M. A. Chamam, G. Laurenczy, S. Das and P. J. Dyson, *Angew. Chem., Int. Ed.*, 2017, **56**, 10559–10563.
32 Y. Wu, Y. Zhao, R. Li, B. Yu, Y. Chen, X. Liu, C. Wu, X. Luo and Z. Liu, *ACS Catal.*, 2017, **7**, 6251–6255.
33 Q.-W. Song, Z.-H. Zhou and L.-N. He, *Green Chem.*, 2017, **19**, 3707–3728.
34 F. Wu, Y. Wang, Y. Zhao, M. Tang, W. Zeng, Y. Wang, X. Chang, J. Xiang, B. Han and Z. Liu, *Sci. Adv.*, 2023, **9**, eade7971.
35 H. Wang, Y. Wu, Y. Zhao and Z. Liu, *Acta Phys.-Chim. Sin.*, 2021, **37**, 2010022.
36 W. Lu, J. Ma, J. Hu, J. Song, Z. Zhang, G. Yang and B. Han, *Green Chem.*, 2014, **16**, 221–225.
37 Y. Zhao, B. Yu, Z. Yang, H. Zhang, L. Hao, X. Gao and Z. Liu, *Angew. Chem., Int. Ed.*, 2014, **53**, 5922–5925.
38 M. Liu, Z. Zhang, H. Liu, Z. Xie, Q. Mei and B. Han, *Sci. Adv.*, 2018, **4**, eaas9319.
39 H. Wang, Y. Zhao, F. Zhang, Z. Ke, B. Han, J. Xiang, Z. Wang and Z. Liu, *Sci. Adv.*, 2021, **7**, eabg0396.
40 D. A. Decato, A. M. S. Riel, J. H. May, V. S. Bryantsev and O. B. Berryman, *Angew. Chem., Int. Ed.*, 2021, **60**, 3685–3692.
41 R. R. Annapureddy, F. Burg, J. Gramüller, T. P. Golub, C. Merten, S. M. Huber and T. Bach, *Angew. Chem., Int. Ed.*, 2021, **133**, 7999–8005.
42 R. A. Sheldon, *Green Chem.*, 2017, **19**, 18–43.
43 T. Lu and F. Chen, *J. Comput. Chem.*, 2012, **33**, 580–592.
44 S. Wu, W. Zhang, L. Qi, Y. Ren and H. Ma, *J. Mol. Struct.*, 2019, **1197**, 171–182.
45 J. Zhang, *J. Chem. Theory Comput.*, 2018, **14**, 572–587.
46 S. M. Banik, A. Levina, A. M. Hyde and E. N. Jacobsen, *Science*, 2017, **358**, 761–764.